MATERIAL CHARACTERIZATION OF A β-Ga$_2$O$_3$ CRYSTAL

Mikhail A. Bryushinin[1*], Igor A. Sokolov[1], Roman V. Pisarev[1],

Anatoly M. Balbashov[2]

[1]Ioffe Physical Technical Institute, Polytekhnicheskaya 26, 194021 St. Petersburg, Russia

[2]Moscow Power Engineering Institute, Krasnokazarmennaya 14, 111250 Moscow, Russia

e-mail: mb@mail.ioffe.ru

Abstract. We report the excitation of the non-steady-state photo-electromotive force in a monoclinic gallium oxide crystal. The crystal grown in an excess of oxygen is insulating and very transparent for a visible light, but this, however, does not prevent us from the formation of dynamic space-charge gratings and observation of the photo-EMF signal at λ=532 nm. The induced ac current is studied for the cases of zero external electric fields. The dependencies of the signal amplitude versus the frequency of phase modulation, light intensity, spatial frequency are measured. The photoconductivity and diffusion length of electrons are estimated for the chosen light wavelength.

1. Introduction

The investigation of transport properties in high-resistive semiconductors is often complicated not only by the small values of electric current, diffusion and drift lengths but also by the formation of the space charge near blocking contact. An elegant solution of this problem was proposed several decades ago, when the non-steady-state photo-EMF effect, or nonstationary holographic current in other terminology, was discovered [1–3]. The effect reveals itself as an alternating electric current arising in a semiconductor illuminated by an oscillating interference pattern. The related techniques realized with an interference pattern running with constant velocity are called as holographic current [4] or moving photocarrier grating technique [5]. The space charge formation produces no harmful action on these effects, on the contrary, it takes part in the excitation of the signal: the resulting electric current appears due to spatial shifts of the space-charge and photoconductivity distributions in the crystal volume. The excitation of the non-steady-state photo-EMF signal involves processes of carrier generation, diffusion and drift in an electric field, recombination to local centers. This complex nature of the effect makes it a powerful tool for determination of photoelectric parameters such as type and value of photoconductivity, carrier lifetime, mobility and diffusion length, density of recombination centers, etc. [3, 5–10]. Besides the tasks of material characterization the non-steady-state photo-EMF is also used for the detection of phase- and frequency-modulated optical signals [11–15]. In this work, we apply the non-steady-state photo-EMF technique for the investigations of a β-Ga$_2$O$_3$ crystal. The combination of the optical and electrical properties of this material attracts the attention of researchers during last years. The band gap of β-Ga$_2$O$_3$ is of 4.8 eV, so the crystal is almost transparent for the visible light. This advances the development of solar-blind detectors of deep ultraviolet radiation based on nanowires [16] and nanobelts [17], thin films [18] or bulk crystals [19].

Oxygen vacancies endow a β-Ga$_2$O$_3$ crystal with the electronic conductivity, and this can be utilized in the fabrication of transparent electrodes [20]. The refractive index of 1.9 can make such electrodes deposited on A3B5 semiconductors to be antireflective [21]. The crystal possess the photocatalytic properties and can be used as a photoelectrode for the water splitting under UV radiation [22]. The application of the material for the development of field-effect transistors and gas sensors was also proposed [23–25]. In spite of the great interest to its ultraviolet applications β-Ga$_2$O$_3$ crystal may still be useful in the visible and even infrared range. Here we shall study the photoelectric properties at λ=532 nm ($h\nu$ =2.33 eV) and try to reveal the material's anisotropy measuring the signal along [100] and [010] axes.

2. Experimental arrangements

The experiments with the excitation of the non-steady-state photo-EMF in β-Ga$_2$O$_3$ are carried out with the arrangement (Fig. 1) used earlier for investigations of other wide-bandgap semiconductors and nanostructured materials [9, 10]. The second harmonic of Nd:YAG laser with the wavelength of λ=532 nm is split into two beams, which then create the interference pattern with spatial frequency K, contrast m=0.98 and average intensity I_0 on the crystal surface. The electro-optic modulator introduces phase modulation with amplitude $\delta = 0.61$ and frequency ω into the signal beam. The photocurrent arising in the sample produces a voltage across the
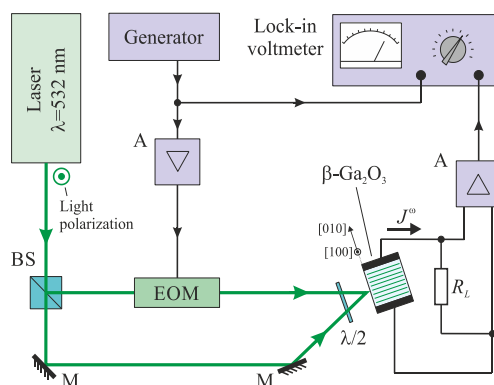

Fig. 1. Experimental setup for the investigation of the non-steady-state photo-EMF. EOM is the electrooptic modulator, BS is the beamsplitter, M is the mirror, A is the amplifier.

load resistor, which was amplified and then measured by the lock-in voltmeter. The polarization plane containing electric field vector is perpendicular to the incidence plane (TE-polarization) in the most of the experiments. The placement of the half-wave plate in front of the sample allows the rotation of the polarization plane, when it is necessary.

β-Ga$_2$O$_3$ is a monoclinic crystal with the cell dimensions a=2.23 Å, b=3.04 Å, c=5.80 Å and β=103.7° [26]. The band gap is indirect with E_g=4.84 eV [27]. The static dielectric constant of the material is a tensor with eigenvalues ε_{11}=10.84, ε_{22}=11.49 and ε_{33}=13.89 [28]. The crystal of gallium oxide was grown by the floating zone method at URN-2-ZM machine produced in Moscow Power Engineering Institute. The single crystal was grown from the ceramic bar obtained by the conventional technology. The seed was oriented so that the crystal grew along the [010] direction. The growth rate of 10 mm/h was chosen to ensure the stability of the crystallization processes. The quality of the obtained single crystals depends on the type of the atmosphere and its pressure. The studied crystal was grown in the 60 bar oxygen atmosphere, which provided the highest sample's quality. The sample used in our studies has the dimensions of 2.00×2.15×1.35 mm along the crystallographic directions [100], [010] and direction perpendicular to the plane (001), respectively. The front and back surfaces

(2.00×2.15 mm) are the (001) crystal's cleaved facets, no additional treatment was applied to them. The silver paste electrodes are deposited on the opposite pairs of lateral surfaces in the experiments with the light pattern grating vector **K**//[100] and **K**//[010].

3. Experimental results

The typical signal amplitude is of $10^{-12} - 10^{-9}$ A, which is two orders of magnitude lower than the values observed in model sillenite crystals $Bi_{12}Si(Ti)O_{20}$ [2, 29]. Nevertheless such an amplitude is sufficient for the detection with the signal-to-noise ratio of 0 - 60 dB. The phase of the signal clearly points to the electron type of photoconductivity.

We have measured the frequency transfer functions of the non-steady-state photo-EMF amplitude in the as fabricated β-Ga_2O_3 crystal (Fig. 2). The dependencies contain the growth of the signal at low frequencies of phase modulation ω followed by the frequency independent part. The signal growth for low frequencies of phase modulation is an important manifestation of the adaptivity of space charge formation in photoconductive materials [2, 30]. The signal at low ω is small because of the fact, that both the space charge field grating and the grating of free electrons (photoconductivity grating) follow the movement of the interference pattern. The spatial shift between them is nearly equal to $\pi/2$, which finally results in small value of the average drift component of the current. The grating with larger relaxation time becomes "frozen-in" at higher frequencies, the spatial shifts between gratings increase, and holographic current reaches its maximum at the frequency-independent region. Since there is no decaying part in the dependence, the space charge formation occurs in the condition of quasi-stationary photoconductivity ($\omega\tau<<1$), and the signal behavior is described by an expression [2]:

$$j^{\omega} = \frac{m^2 \Delta\sigma_0 E_D}{2} \frac{-i\omega\tau_M}{1+i\omega\tau_M(1+K^2 L_D^2)} . \tag{1}$$

Here $E_D=(k_B T/e)$ is the diffusion field, k_B is the Boltzmann constant, T is the temperature, e is the electron charge, $\tau_M=\varepsilon\varepsilon_0/\sigma_0$ is the Maxwell relaxation time, σ_0 is the average conductivity and L_D is the diffusion length of electrons [30]. The growing and frequency-independent regions are separated by the cut-off frequency ω_1:

$$\omega_1=[\tau_M(1+K^2 L_D^2)]^{-1}. \tag{2}$$

The dependencies of the signal amplitude and the first cut-off frequency versus illumination level are presented in Fig. 3.

The amplitude of the photocurrent in the maximum of frequency transfer function is proportional to the light intensity: $J^{\omega} \propto I_0$. There is, however, a sublinear dependence of the cut-off frequency $\omega_1 \propto I_0^{0.69}$ for **K**//[100] and $\omega_1 \propto I_0^{0.51}$ for **K**//[010]. This can be due to the corresponding nonlinearity of the photoconductivity. The presence of dark conductivity can contribute in the initial stage of dependence $\omega_1(I_0)$ as well. As seen from Eq. (2) the measurements of the cut-off frequency ω_1 at low K provide the estimate of the Maxwell relaxation time and corresponding photoconductivity of the sample. For the chosen intensities $I_0=0.039 - 0.40$ W/cm^2 of TE-polarized light the photoconductivity equals $\sigma_0 = (0.48 - 2.5)\times10^{-10}$ Ω^{-1}cm^{-1} along the [100] axis and $\sigma_0 = (0.32 - 1.0)\times10^{-10}$ Ω^{-1}cm^{-1} along the [010] axis.

Dependence of the signal amplitude on the spatial frequency of the interference pattern is another characteristic usually measured in the non-steady-state photo-EMF experiments (Fig. 4).

The observed behavior of the signal is explained as follows: the growth of the signal at low K is due to the increase of the space charge field amplitude, which is proportional to the diffusion field E_D [30]. The decay at high K is caused by the diffusion "blurring" of the

photoconductivity grating. The expression for this dependence is known from the theory of the non-steady-state photo-EMF effect [2, 3]:

$$J^{\omega} \propto \frac{K}{1 + K^2 L_D^2} \cdot$$ (3)

The maximum of the signal is achieved at $K = L_D^{-1}$, so the electron diffusion length can easily be estimated from the experimental curves: $L_D = 190$ nm for $\mathbf{K}//[100]$ and $L_D = 200$ nm for $\mathbf{K}//[010]$. Figure 4 also presents the dependencies of the first cut-off frequency versus spatial frequency. These dependencies are fitted using Eq. (2) with $L_D = 110$ nm for $\mathbf{K}//[100]$ and $L_D = 130$ nm for $\mathbf{K}//[010]$. We should note that increased light reflection at large incident angles leads to the decrease of the light intensity in the crystal volume, and this can affect the signal excitation for $K > 10$ μm^{-1}. The difference in the estimates of the diffusion length obtained from dependencies $J^{\omega}(K)$ and $\omega_1(K)$ may be associated with the mentioned factor.
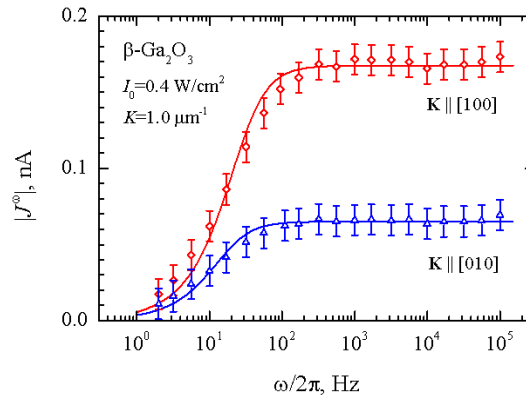

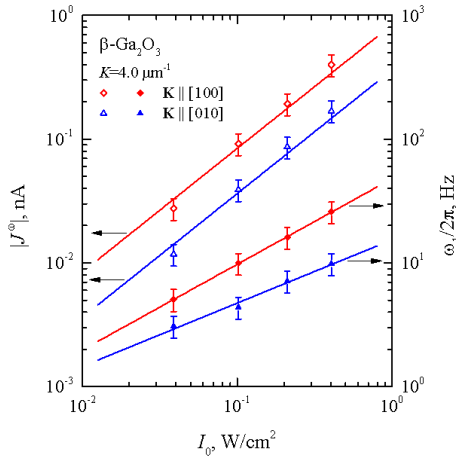**Fig. 2.** Frequency transfer functions of the non-steady-state photo-EMF J^{ω} measured for two crystal orientations.

Fig. 3. Dependencies of the signal amplitude J^{ω} and the first cut-off frequency ω_1 versus average light intensity.
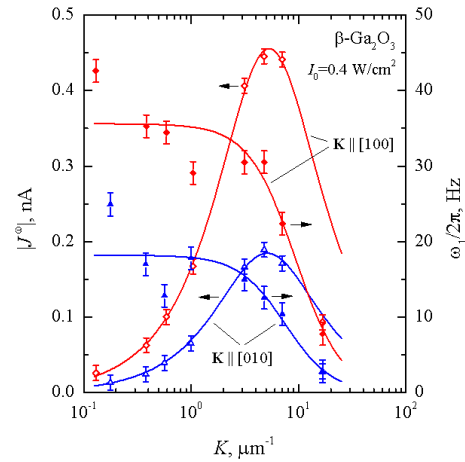

Fig. 4. Dependencies of the signal amplitude J^{ω} and the first cut-off frequency ω_1 versus spatial frequency K of the interference pattern.

4. Discussion and conclusion.

The studied Ga_2O_3 crystal has some advantages over the mentioned $Bi_{12}SiO_{20}$ crystal. The frequency transfer function of the former is flat in the range of 0.1-100 kHz, while the signal in the latter decays over 10 kHz. Moreover, the additional measurements of the photoconductivity relaxation in the Ga_2O_3 crystal allow us to state that the frequency dependence should be flat up to 600 kHz. This means that the photoconductivity relaxation time, which is equal to the

electron lifetime in the simplest case, should not exceed 0.26 µs. No influence of shallow traps has been revealed (compare Fig. 2 with those in Refs. [9, 10]). The material has a moderate static dielectric constant ε=10, which is about 5 times lower than that in sillenite crystals, and this allows to achieve the appropriate cut-off frequency for low illumination levels. The signal-to-noise ratio is up to 60 dB for the amplitude of phase modulation $\delta = 0.61$ and nearly equal light intensities of the signal and reference beams (m=0.98). For such experimental conditions the minimum vibration amplitude to be detected by adaptive photodetector using Ga_2O_3 crystal is $x_{min} \approx 2.6 \times 10^{-11}$ m (detection bandwidth Δf=1 Hz).

In conclusion, we have demonstrated the capabilities of the non-steady-state photo-EMF technique in characterization of the wide-bandgap monoclinic Ga_2O_3 crystal. The signal was studied in the absence of an external dc electric field. The photoelectric parameters such as photoconductivity and diffusion length of electrons are estimated. The rather high amplitude of the signal and flatness of the frequency response in Ga_2O_3 makes this crystal a good candidate for the production of adaptive sensors for vibration and stress measurement.

References
[1] G.S. Trofimov, S.I. Stepanov // *Soviet Physics-Solid State* **28** (1986) 1559.
[2] M.P. Petrov, I.A. Sokolov, S.I. Stepanov, G.S. Trofimov // *Journal of Applied Physics* **68** (1990) 2216.
[3] I.A. Sokolov, S.I. Stepanov // *Journal of the Optical Society of America B* **10** (1993) 1483.
[4] N.V. Kukhtarev, T. Kukhtareva, S.F. Lyuksyutov, M.A. Reagan, P.P. Banerjee, P. Buchhave // *Journal of the Optical Society of America B* **22** (2005) 1917.
[5] U. Haken, M. Hundhausen, L. Ley // *Physical Review B* **51** (1995) 10579.
[6] H. Veenhuis, K. Buse, E. Krätzig, N. Korneev, D. Mayorga // *Journal of Applied Physics* **86** (1999) 2389.
[7] M.C. Gather, S. Mansurova, K. Meerholz // *Physical Review B* **75** (2007) 165203.
[8] T. O. dos Santos, J. Frejlich, K. Shcherbin // *Applied Physics B* **99**, (2010) 701.
[9] M.A. Bryushinin, V.V. Kulikov, E.V. Mokrushina, E.N. Mokhov, A.A. Petrov, I.A. Sokolov // *Journal of Physics D: Applied Physics* **47** (2014) 415102.
[10] M.A. Bryushinin, A.A. Petrov, R.V. Pisarev, I.A. Sokolov // *Physics of the Solid State* **57** (2015) 907.
[11] S.I. Stepanov, I.A. Sokolov, G.S. Trofimov, V.I. Vlad, D. Popa, I. Apostol // *Optics Letters* **15** (1990)1239.
[12] M.A. Bryushinin, K.T.V. Grattan, V.V. Kulikov, I.A. Sokolov // *Journal of Modern Optics* **53** (2006) 857.
[13] T. dos Santos, J. Frejlich, J. Launay, K. Shcherbin // *Applied Physics B* **95** (2009) 627.
[14] S. Mansurova, P. Moreno Zarate, P. Rodriguez, S. Stepanov, S. Kober, K. Meerholz // *Optics Letters* **37** (2012) 383.
[15] M. Bryushinin, V. Kulikov, I. Sokolov, P. Delaye, G. Pauliat // *EPL – Europhysics Letters* **105** (2014) 64003.
[16] P. Feng, J.Y. Zhang, Q.H. Li, T.H. Wang // *Applied Physics Letters* **88** (2006) 153107.
[17] L. Li, E. Auer, M. Liao, X. Fang, T. Zhai, U. K. Gautam, A. Lugstein, Y. Koide, Y. Bandoa, D. Golberga // *Nanoscale* **3** (2011) 1120.
[18] Y. Kokubun, K. Miura, F. Endo, S. Nakagomi // *Applied Physics Letters* **90** (2007) 031912.
[19] T. Oshima, T. Okuno, N. Arai, N. Suzuki, S. Ohira, S. Fujita // *Applied Physics Express* **1** (2008) 011202.

[20] M. Orita, H. Ohta, M. Hirano, H. Hosono // *Applied Physics Letters* **77** (2000) 4166.

[21] M. Passlack, E.F. Schubert, W.S. Hobson, M. Hong, N. Moriya, S.N.G. Chu, K. Konstadinidis, J.P. Mannaerts, L. Schnoes, G.J. Zydzik // *Journal of Applied Physics* **77** (1995) 686.

[22] T. Oshima, K. Kaminaga, H. Mashiko, A. Mukai, K. Sasaki, T. Masui, A. Kuramata, S. Yamakoshi, A. Ohtomo // *Japanese Journal of Applied Physics* **52** (2013) 111102 .

[23] P.-C. Chang, Z. Fan, W.-Y. Tseng, A. Rajagopal, J.G. Lu // *Applied Physics Letters* **87** (2005) 222102.

[24] M. Higashiwaki, K. Sasaki, A. Kuramata, T. Masui, S. Yamakoshi // *Applied Physics Letters* **100** (2012) 013504.

[25] M. Fleischer, H. Meixner // *Sensors & Actuators, B: Chemical* **5** (1991) 115–119.

[26] S. Geller // *The Journal of Chemical Physics* **33** (1960) 676.

[27] H. Peelaers, C.G. Van de Walle // *Physica Status Solidi B* **252** (2015) 828.

[28] B. Liu, M. Gu, X. Liu // *Applied Physics Letters* **91** (2007) 172102.

[29] M. Bryushinin, V. Kulikov, I. Sokolov // *Physical Review B* **67** (2003) 075202.

[30] M.P. Petrov, S.I. Stepanov, A.V. Khomenko, In: *Springer Series in Optical Sciences* (Springer-Verlag, Berlin Heidelberg, 1991), Vol. 59.